NANO LETTERS

pubs.acs.org/NanoLett

Combined Surface Plasmon and Classical Waveguiding through Metamaterial Fiber Design

Elliot J. Smith,*,† Zhaowei Liu,‡ Yongfeng Mei,*,† and Oliver G. Schmidt†

†Institute for Integrative Nanosciences, IFW Dresden, Helmholtzstrasse 20, D-01069 Dresden, Germany, and
‡Electrical & Computer Engineering, University of California, San Diego, 9500 Gilman Drive, La Jolla, California 92093

ABSTRACT A metamaterial integration for fiber optics, leading to a dual effect of surface plasmon and classical waveguiding, is presented along with experimental potentiality. We theoretically propose a metamaterial fiber in which, depending on the wavelength (from ultraviolet to infrared) and the particular metamaterial composition, one can transmit information through surface plasmon mediated or classical waveguidance. The metamaterial can be used as the core or cladding of a fiber which allows waveguidance through a subwavelength geometry.

KEYWORDS Surface plasmon, optical fiber, metamaterial, tunable cladding

The theoretical and experimental work on metamaterials has led to numerous potential applications including cloaking devices,[1] subdiffraction limited imaging,[2−6] and two-dimensional (2D) surface plasmon (SP) waveguides.[7] SP waveguides are one important topic because of their capability in transmitting subwavelength information,[7] which could give way to faster, more compact optoelectronic communications and sensors.[8] Nanotechnology allows for the creation of new material properties which cannot be found in nature,[1−6,9−14] and these materials have been referred to as metamaterials. For instance, materials exhibiting negative index of refraction, so-called "left-handed" metamaterials named for the characteristic property of acting in an opposite manner of the right-hand rule, cause interesting phenomena like nonclassical bending of light.[9−12] Negative index of refraction (n) was first theoretically proposed by Veselago in 1968, who suggested that an anisotropic material could, with simultaneous negative permeability μ and permittivity ε, yield negative refractive properties.[9] Negative index mediums (NIM) have been experimentally demonstrated from the microwave to visible spectral range.[10−13] Still, the NIM at visible frequencies is mainly at a level of material property demonstration. The material itself has a number of limitations to be used in practice such as significant resonant loss and the difficulties to fabricate bulky materials with 3D fine structures. However, for a plasmonic metamaterial, only the permittivity needs to be considered, which considerably alleviates the challenges mentioned above. As a result, such materials have been used to demonstrate various devices at optical, even visible frequencies.[2−7]

* Corresponding authors, e.j.smith@ifw-dresden.de and y.mei@ifw-dresden.de.
Received for review: 02/20/2009
Published on Web: 04/15/2009

Classical core propagation waveguides have been subject to important studies over the last century and include subcategories of fiber sensors and communication devices. Fiber waveguides have also been explored using concepts like Bragg fibers; which have a cladding made up of alternating layers of different dielectric materials leading to low loss single mode fibers,[15,16] with potential use in telecommunication and sensors for chemical, temperature, and gas detection.[17] The industry standard for solid core, single mode fiber optics consists of using a silica glass based core/cladding (Figure 1a) combination which leads to low-loss light transmission. Research has been focused on other designs for waveguiding including negative dielectric optical waveguides for nano-optical guiding[18] and hollow waveguiding because of advantages in laser light delivery systems, low insertion loss, no end reflection, and small beam divergence.[17] For instance, the idea of using nanosized metal waveguides has been explored for light propagation; due to the negative permittivities of some metals in the visible spectral range, light can propagate through subwavelength nanopins.[18] Research in hollow waveguides has resulted in many developments including attenuated total reflectance guides (ATR, $n < 1$) (i.e., sapphire at the wavelength of 10.6 μm),[19] and photonic band gap guides[20] (Figure 1b).

In this Letter we propose a way in which plasmonic metamaterials open the door for a new type of waveguide, one that could be used for Leaky, ATR, and SP guidance (Figure 1c). Such a fiber design creates more versatility due to its dispersive characteristics compared to materials found naturally. Depending on the wavelength and material composition, different mode profiles can propagate through such a fiber. Figure 1c.1 shows the effect of having a subwavelength metamaterial cladding design of a fiber allowing the propagation of light through hollow core guidance. The

DOI: 10.1021/nl900550j | *Nano Lett.* **2010,** *10,* 1-5

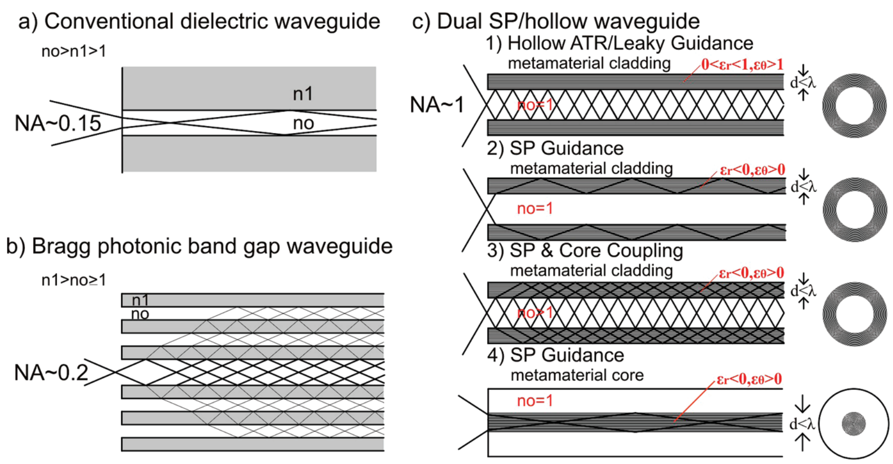

FIGURE 1. (a) A ray diagram for a conventional, solid core, silicon-based dielectric waveguide. (b) A ray diagram representing the mechanism in which a Bragg photonic band gap waveguide works through Bragg reflection of light, leading to propagation through the core. (c.1−3) A ray diagram for a fiber using a metamaterial as cladding. Given the dispersive characteristics of the metamaterial, one can tune between core propagation (c.1) or surface plasmon propagation in the metamaterial cladding (c.2). (c.3) Shows the combined coupling of surface plasmon modes with classical core modes that occurs when a liquid or gas is introduced into the core. (c.4) Propagation of plasmons when the metamaterial is used as the core. Depending on the wavelength, and material makeup, light can be guided with this special fiber utilizing component geometries smaller than the incident wavelength and can propagate light using attenuated total reflectance, leaky, or surface plasmon guidance.

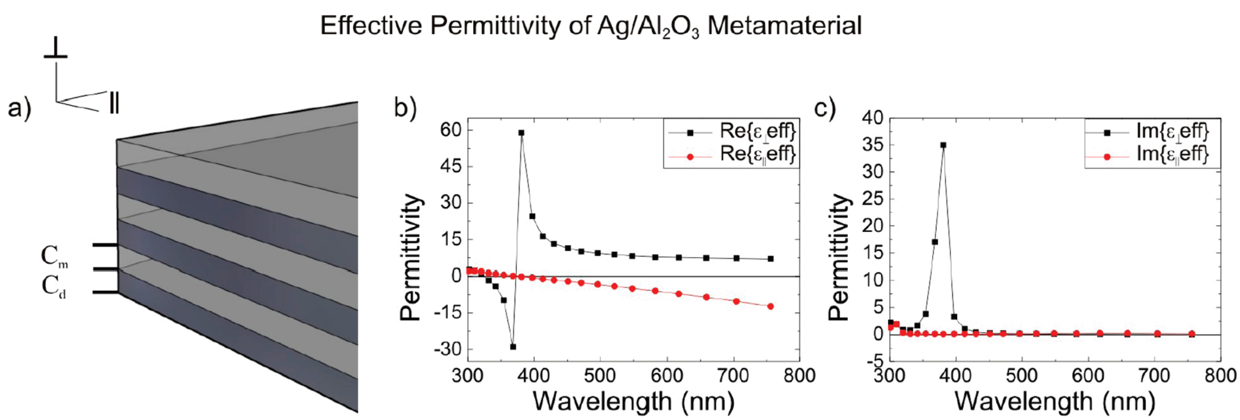

FIGURE 2. When stacked thin films of different materials are deposited, and their combined bilayer thickness $d \ll \lambda$, then the effective permittivities of the system as a whole can be calculated. (a) A lattice diagram of the structure of metamaterial studied. C_d and C_m are ratios of the thickness of the metal and dielectric layer to one another, where $C_d + C_m = 1$. The parallel direction is in the plane of the stacks (direction of light guidance) the perpendicular direction points out of the stack. (b) The calculated real part of the perpendicular and parallel component of the effective permittivity for a Ag/Al_2O_3 lattice ($C_d = {}^1/_2$, $C_m = {}^1/_2$). (c) The corresponding calculated imaginary part of the perpendicular and parallel component of the effective permittivity.

wavelength or materials can be changed to shift the permittivity of the cladding, giving way to plasmonic propagation in the cladding, Figure 1c.2. When a liquid or gas is placed inside the core, a coupling of plasmonic modes and classical modes can be observed, Figure 1c.3. A metamaterial can also be used as the core of a fiber, permitting the use of subwavelength core guidance, Figure 1c.4.

Careful metamaterial design enables deliberate tuning of the effective permittivities of the cladding or core of a fiber. A metamaterial design makes it possible to use subwavelength layered claddings and cores. The cladding or core can be smaller than the incident wavelength and still propagate light in the form of surface plasmons; classical waveguides are limited to being larger than the incoming wavelength, for single mode guidance usually on the order of 10 and 125 μm for the core and cladding, respectively,[21] and larger for multimode guidance. A classical single mode fiber also lacks from its low numerical aperture, NA $= n_0[2(n_0 - n_1)/n_0]^{1/2}$ (ref 21), of NA $\sim$ 0.15. Through nanotechnology, band gap photonic fibers have been developed which have the advantage of guidance in air but the overall geometry is comparable to classical wave guidance with an inner radius of $\sim$15 μm and a cladding layer of $\sim$100 μm[20] (later work from the same group reported a NA $\sim$ 0.28 using a solid core[22]). Integrating a metamaterial into a fiber optic design not only allows the ability to have Leaky, ATR, and SP guidance but also permits an overall smaller geometry, with a cladding thickness on the order of 40−500 nm, a subwavelength core, and a NA approaching unit.

This fiber optic integration provides many degrees of freedom, making the desired permittivity obtainable by changing the wavelength, materials and their relative thicknesses. Our material design is composed of alternating layers of a metal and an oxide, which can produce an anisotropic plasmonic metamaterial.[2−6] The materials focused on in this Letter are Al_2O_3/Ag; however other material combinations are also possible (material parameters for Ag and Al_2O_3 taken from refs 23 and 24). A planar depiction of the setup is given in Figure 2a. We assume $\mu = 1$ and we look at a variance in the ε of the material. When the individual metal−oxide bilayer thickness is much smaller than the wavelength, an effective permittivity can be calculated,[25] given by

$$\varepsilon_\perp^{\text{eff}} = \frac{(c_m + c_d)\varepsilon_m\varepsilon_d}{c_d\varepsilon_m + c_m\varepsilon_d} \tag{1}$$

$$\varepsilon_\parallel^{\text{eff}} = \frac{c_m\varepsilon_m + c_d\varepsilon_d}{c_m + c_d} \tag{2}$$

where $\varepsilon_\perp^{\text{eff}}$ and $\varepsilon_\parallel^{\text{eff}}$ are the effective perpendicular and parallel permittivities of the material, respectively, for a cross section of the stacked layers, Figure 2a; c_m and c_d are the proportional ratios for the bilayer thickness of the metal and dielectric layers, $c_m + c_d = 1$. The calculated $\varepsilon_\perp^{\text{eff}}$ and $\varepsilon_\parallel^{\text{eff}}$ for a Al_2O_3/Ag multistacked bilayer of equal thicknesses is given in Figure 2, parts b and c. Equations 1 and 2 are an idealized approximation, whose accuracy improves for a large number of bilayers. This metamaterial composition, at particular wavelengths, leads to the anisotropy needed for a plasmonic material.[2−6]

The calculation for the effective permittivity allows us to simulate a material with an anisotropic effective permittivity (eq 3), greatly simplifying the geometry and time needed for simulation, or

$$[\varepsilon^{\text{eff}}] = \begin{bmatrix} \varepsilon_\perp \cos^2(\phi) + \varepsilon_\parallel \sin^2(\phi) & (\varepsilon_\perp - \varepsilon_\parallel)\sin(\phi)\cos(\phi) & 0 \\ (\varepsilon_\perp - \varepsilon_\parallel)\sin(\phi)\cos(\phi) & \varepsilon_\perp \sin^2(\phi) + \varepsilon_\parallel \cos^2(\phi) & 0 \\ 0 & 0 & \varepsilon_\parallel \end{bmatrix} \tag{3}$$

Equation 3, given in Cartesian coordinates, takes into account the coordinate conversion for the permittivity tensor going from a planar stacked structure to that of a rolled one, showing that this material composition leads to a 3-fold ($\hat{r}$, $\hat{\phi}$, $\hat{z}$) anisotropy for the metamaterial. This approximation is later justified by the simulations where a rolled-up metal/oxide bilayer displays similar mode profiles. According to our calculations, there are five regions of interest with this metamaterial design. Using the plots from Figure 2b, we simulated an idealized (neglecting material loss) hollow waveguide made from an anisotropic material. There are a number of regions in which the permittivities of our system have unique values, Figure 3b: ($\varepsilon_\parallel^{\text{eff}} < 0/\varepsilon_\perp^{\text{eff}} > 0$) ($\varepsilon_\parallel^{\text{eff}} > 0/\varepsilon_\perp^{\text{eff}} < 0$) ($\varepsilon_\parallel^{\text{eff}} > 0/\varepsilon_\perp^{\text{eff}} > 0$) ($0 < \{\varepsilon_\parallel^{\text{eff}}, \varepsilon_\perp^{\text{eff}}\} < 1$) ($\varepsilon_\parallel^{\text{eff}}/\varepsilon_\perp^{\text{eff}} = 0$). The region where $\varepsilon_\parallel^{\text{eff}}$ and $\varepsilon_\perp^{\text{eff}}$ are both negative arises from guides made of metal[18] and will not be discussed here.

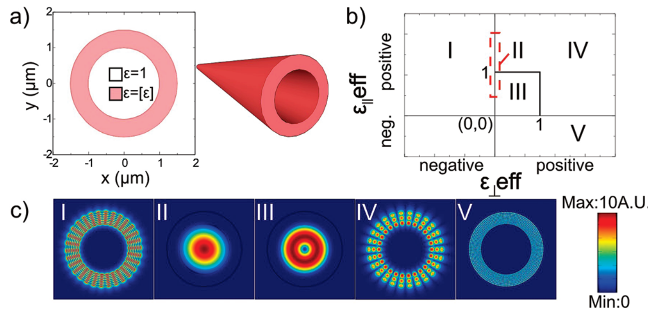

FIGURE 3. A layout showing the different wavelength-dependent regions of interest for investigation for different material compositions is presented. (a) The geometry of our design where we use a hollow waveguide in air with an inner radius of 2 μm and a cladding thickness of 500 nm. (b) The different regions of effective permittivities, which we can achieve with our anisotropic metamaterial (the region in which both perpendicular and parallel permittivities are negative for an effective anisotropic metal will not be discussed here). (c) An example from each of the regions shown in (b). Region I is when $\varepsilon_\parallel^{\text{eff}}$ is positive and $\varepsilon_\perp^{\text{eff}}$ is negative, which can propagate surface plasmons. Region IV ($\varepsilon_\parallel^{\text{eff}} > 0/\varepsilon_\perp^{\text{eff}} > 0$) and region V ($\varepsilon_\parallel^{\text{eff}} < 0/\varepsilon_\perp^{\text{eff}} > 0$) also allow for the propagation of surface plasmons. Region II shows hollow ATR waveguidance as the perpendicular effective permittivity approaches zero from the positive and minus side. Region III is an area of ATR propagation, where both effective permittivities are between 0 and 1.

We investigate a hollow waveguide with an inner radius of 2 μm, integrating a metamaterial as the cladding layer with a thickness of 500 nm, for a total diameter of 3 μm. With the simplification of eq 3 we take a 2D cross section of the waveguide as shown in Figure 3a and set our effective cladding permittivity to the different regions of anisotropy which arise in our system, using realistic values from eqs 1 and 2 for a given wavelength. With the finite element method program COMSOL, we solve for the magnetic field using the modal eigenvalue solver and search for hybrid modes (modes which have both electric and magnetic field components in the direction of propagation) at the desired effective permittivity. Shown in Figure 3c, are a few examples of the magnetic field distribution for the many modes that are excited in our waveguide for the various regions. Region III is the region in which the cladding has effective permittivities between 0 and 1, which leads to ATR guidance. As the perpendicular component of the effective permittivity approaches 0, from the negative and positive sides, the fiber continues to guide the light classically (Figure 3c.II). The anisotropic and negative characterizations of the other regions allow for bulk plasmonic guidance in the cladding (Figure 3c.I,IV,V), where region V supports higher order modes than region I and region I supports higher order modes than region IV.

Surface plasmon propagation length and, in turn, loss arising in SP waveguides is attributed to the absorption of the metal, coming from the imaginary part of the complex permittivity. Attenuation in the metamaterial fiber can be evaluated by using the effective media theory. The propagation wave is influenced by the parallel effective permittivity in our guide; because of this, the imaginary part of $\varepsilon_\parallel^{\text{eff}}$ is

DOI: 10.1021/nl900550j | *Nano Lett.* **2010,** *10,* 1-5

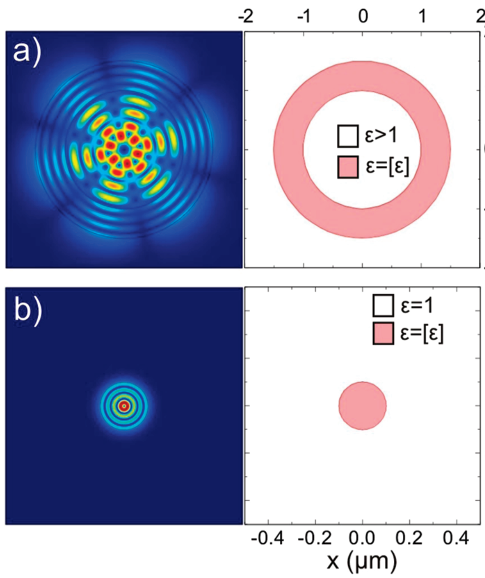

FIGURE 4. (a) With the same geometry from Figure 3 and values from region I, an introduction of a liquid or gas into the core (shown here is methanol, $n = 1.3288$ (index of refraction from ref 29)) leads to an effect of coupled plasmonic and classical modes. In (b) a metamaterial core smaller than the incident wavelength (here the core has a diameter of 200 nm and the incident wavelength is 342 nm) can act as a conventional multimode fiber. The fiber can be smaller than the incoming wave and still support the propagating mode.

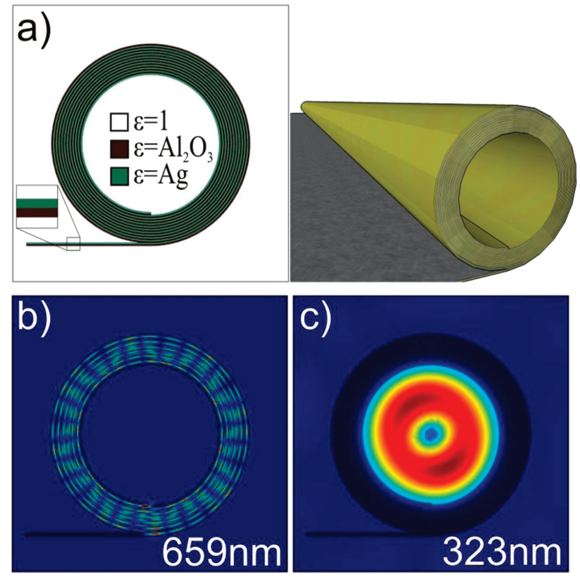

FIGURE 5. Simulations for a rolled-up Al_2O_3/Ag bilayer hollow/SP waveguide are presented. (a) The geometry of a cross section for rolled-up bilayer surrounded by air. The rolled-up bilayer is comparable to a hollow cylinder with an effective anisotropic material. (b) Bulk plasmonic mode propagation. (c) Classical hollow waveguiding due to an effective permittivity between 0 and 1.

what is responsible for attenuated propagation for SP modes in the metamaterial. $\mathrm{Im}\{\varepsilon_{\parallel}^{\mathrm{eff}}\}$ is linearly proportional to $\mathrm{Im}\{\varepsilon_{\mathrm{m}}\}$; for a 1:1 ratio of Al_2O_3 and Ag in the spectral range shown in Figure 2c, the linearity constant is approximately 0.5, suggesting that the fiber will have a longer propagation length than 2D SP waveguides consisting of a single strip of metal sandwiched between two oxides. The imaginary part of $\varepsilon_{\parallel}^{\mathrm{eff}}$ can be decreased with a higher ratio of oxide to metal, thereby decreasing the attenuation.

Other groups have explored the use of surface plasmons as smaller, improved sensors being capable of providing subwavelength information of a system.[8] Taking our design and introducing a gas or liquid into the core of the waveguide leads to a coupling of the classical core and bulk plasmonic cladding modes (Figure 4a) suggesting the utilization of such a metamaterial fiber as a gas or chemical detector. The coupling of the plasmonic and core modes could provide transmission of subwavelength information of the liquid or gas, which in turn would give way to more sensitive sensors.

A simulated demonstration of the effect of using a subwavelength metamaterial core, Figure 1c.4, is shown in Figure 4b. This geometry benefits from the ability to guide light with a core smaller than that of the incident wavelength, which is a major disadvantage of classical fibers. These smaller geometries could provide further miniaturization of optoelectronic components.

From a 2D side view approach of our fiber (Figure 1c), an evaluation can be made for the numerical aperture of a metamaterial cladding. The NA comes from the fact that for the total internal reflection necessary for guidance, the incident angle of light must be larger than that of the critical angle of the material interface, given by $\theta_c = \sin^{-1}(n_{\mathrm{clad}}/n_{\mathrm{core}})$. The index of refraction is defined as $n = (\varepsilon\mu)^{1/2}$; assuming again $\mu_{\mathrm{clad}} = 1$ and an air core, $n_{\mathrm{core}} = 1$, we obtain $\theta_c = \sin^{-1}(\varepsilon_{\mathrm{eff}}^{1/2})$. In regions II and III, where $\varepsilon_{\mathrm{eff}}$ is less than air, the critical angle can be calculated. As $\varepsilon_{\mathrm{eff}}$ approaches 0, the critical angle approaches 0, resulting in the numerical aperture, $\mathrm{NA} = \cos(\theta_c)$, approaching 1. For effective negative permittivities, region I, the result is total internal reflection for nonevanescent waves due to the metal-like properties, also resulting in a numerical aperture approaching unity.

Switching from an idealized effective permittivity to a realizable one, we take a rolled-up structure consisting of a bilayer of Ag and Al_2O_3 with a combined thickness of 40 nm (Figure 5a). This type of microtubular structure is producible via rolled-up nanotechnology,[26,27] and classical waveguiding has been both observed in the near-infrared[28] and proposed for X-rays[30] using such structures. A 2D cross section is taken for this rolled-up structure, and some of the modes which arise are shown in parts b and c of Figure 5. Further analysis on how these modes propagate individually is needed. The modes shown in a realizable structure formed from a rolled-up metal/oxide bilayer (Figure 5) are comparable to the modes found in an idealized structure with an anisotropic effective permittivity shown in Figure 3.

In this Letter we have presented a way of combining classical and SP waveguiding in a single system through the development of a tunable fiber cladding or core composed of a metamaterial. Given the dispersion of the material, a manipulation of different material combinations permits the

DOI: 10.1021/nl900550j | Nano Lett. 2010, 10, 1-5

development of a cladding which makes it possible to have classical waveguiding in the core and SP waveguiding in the cladding using subwavelength geometries. We demonstrated the propagation that occurs in an ideal anisotropic material and compared that to an experimentally obtainable design composed of a rolled-up bilayer of a metal and an oxide. We showed that an introduction of a gas or liquid in the waveguide causes the coupling of modes in the core with those in the cladding, which have the potential to be used as more sensitive sensors.

Acknowledgment. The authors thank A. Kleiner, D. J. Thurmer, S. Kiravittaya, P. Cendula, and R. J. Smith for fruitful discussions.

Note Added after ASAP Publication. This paper was published on the Web on April 15, 2009, with errors in equation 1. The corrected version was reposted on December 17, 2009.

REFERENCES AND NOTES

(1) Cai, W.; Chettiar, U. K.; Kildishev, A. V.; Shalaev, V. M. *Nat. Photonics* **2007**, *1*, 224–227.
(2) Wood, B.; Pendry, J. B. *Phys. Rev. B* **2006**, *74*, 115116.
(3) Liu, Z.; Lee, H.; Xiong, Y.; Sun, C.; Zhang, X. *Science* **2007**, *315*, 1686.
(4) Salandrino, A.; Engheta, N. *Phys. Rev. B* **2006**, *74*, No. 075103.
(5) Lee, H.; Liu, Z.; Xiong, Y.; Sun, C.; Zhang, X. *Opt. Express* **2007**, *15*, 15886.
(6) Xiong, Y.; Liu, Z.; Sun, C.; Zhang, X. *Nano Lett.* **2007**, *7*, 3360–3365.
(7) Barnes, W. L.; Dereux, A.; Ebbesen, T. W. *Nature (London)* **2003**, *424*, 824–830.
(8) Zeng, J.; Liang, D. *J. Intell. Mater. Syst. Struct.* **2006**, *17*, 787–791.
(9) Veselago, V. G. *Sov. Phys. Usp.* **1968**, *10*, 509–514.
(10) Shelby, R. A.; Smith, D. R.; Schultz, S. *Science* **2001**, *292*, 77–79.
(11) Valentine, J.; Zhang, S.; Zentgraf, T.; Ulin-Avila, E.; Genov, D. A.; Bartal, G.; Zhang, X. *Nature (London)* **2008**, *455*, 376–379.
(12) Yao, J.; Liu, Z.; Liu, Y.; Wang, Y.; Sun, C.; Bartal, G.; Stacy, A. M.; Zhang, X. *Science* **2008**, *321*, 930.
(13) Liu, N.; Guo, H.; Fu, L.; Kaiser, S.; Schweizer, H.; Giessen, H. *Nat. Mater.* **2008**, *7*, 31–37.
(14) Rill, M. S.; Plet, C.; Thiel, M.; Staude, I.; Freymann, G. V.; Linden, S.; Wegener, M. *Nat. Mater.* **2008**, *7*, 543–546.
(15) Yeh, P.; Yariv, A. *J. Opt. Soc. Am.* **1978**, *68*, 1196–1201.
(16) Ibanescu, M.; Johnson, S. G.; Soljačić, M.; Joannopoulos, J. D.; Fink, Y.; Weisberg, O.; Engeness, T. D.; Jacobs, S. A.; Skorobogatiy, M. *Phys. Rev. E* **2003**, *67*, 046608.
(17) Harrington, J. A. *Fiber Integr. Opt.* **2000**, *19*, 211–217.
(18) Takahara, J.; Yamagishi, S.; Taki, H.; Morimoto, A.; Kobayashi, T. *Opt. Lett.* **1997**, *22*, 475–477.
(19) Hidaka, T.; Morikawa, T.; Shimada, *J. Appl. Phys.* **1981**, *52*, 4467–4471.
(20) Cregan, R. F.; Mangan, B. J.; Knight, J. C.; Birks, T. A.; Russell, P. St. J.; Roberts, P. J.; Allan, D. C. *Science* **1999**, *285*, 1537–1539.
(21) Sanghera, J. S.; Aggarwal, I. D. *Infrared Fiber Optics*; CRC Press: Boca Raton, FL, 1998.
(22) Argyros, A.; Birks, T. A.; Leon-Saval, S. G.; Cordeiro, C. M. B.; Russell, P. St. J. *Opt. Express* **2005**, *13*, 2503–2511.
(23) Johnson, P. B.; Christy, R. W. *Phys. Rev. B* **1972**, *6*, 4370–4379.
(24) Palik, E. D.; *Handbook of optical constants of solids*; Academic Press: San Diego, CA, 1998.
(25) Rytov, S. M. *Sov. Phys. JETP* **1955**, *29*, 605–616.
(26) Schmidt, O. G.; Eberl, K. *Nature (London)* **2001**, *410*, 168.
(27) Mei, Y. F.; Huang, G. S.; Solovev, A. A.; Bermúdez Ureña, E.; Mönch, I.; Ding, F.; Reindl, T.; Fu, R. K. Y.; Chu, P. K.; Schmidt, O. G. *Adv. Mater.* **2008**, *20*, 4085–4090.
(28) Mendach, S.; Songmuang, R.; Kiravittaya, S.; Rastelli, A.; Benyoucef, M.; Schmidt, O. G. *Appl. Phys. Lett.* **2006**, *88*, 111120.
(29) Lide, D. R. *CRC Handbook of Chemistry and Physics 2003–2004*; CRC Press: Boca Raton, FL, 2003.
(30) Deneke, C. H.; Schmidt, O. G. *Appl. Phys. Lett.* **2006**, *89*, 123121.

DOI: 10.1021/nl900550j | *Nano Lett.* **2010,** *10,* 1-5